Journal of Colloid and Interface Science 614 (2022) 120–129

Contents lists available at ScienceDirect

Journal of Colloid and Interface Science

journal homepage: www.elsevier.com/locate/jcis

MUC5B mucin films under mechanical confinement: A combined neutron reflectometry and atomic force microscopy study

Juan F. Gonzalez-Martinez [a,b,1], Hannah Boyd [a,b,1], Philipp Gutfreund [c], Rebecca J.L. Welbourn [d], Carolina Robertsson [b,e], Claes Wickström [b,e], Thomas Arnebrant [a,b], Robert M. Richardson [f], Stuart W. Prescott [g], Robert Barker [h], Javier Sotres [a,b,*]

[a] Department of Biomedical Science, Malmö University, 20506 Malmö, Sweden
[b] Biofilms-Research Center for Biointerfaces, Malmö University, 20506 Malmö, Sweden
[c] Institut Laue Langevin, 71 avenue des Martyrs, Grenoble 38000, France
[d] ISIS Facility, STFC, Rutherford Appleton Laboratory, Chilton, Didcot, Oxon OX11 0QX, United Kingdom
[e] Department of Oral Biology and Pathology, Malmö University, 20506 Malmö, Sweden
[f] School of Physics, University of Bristol, Tyndall Avenue, BS8 1TL Bristol, United Kingdom
[g] School of Chemical Engineering, University of New South Wales, Sydney, NSW 2052, Australia
[h] School of Physical Sciences, University of Kent, Canterbury, Kent CT2 7NH, United Kingdom

GRAPHICAL ABSTRACT

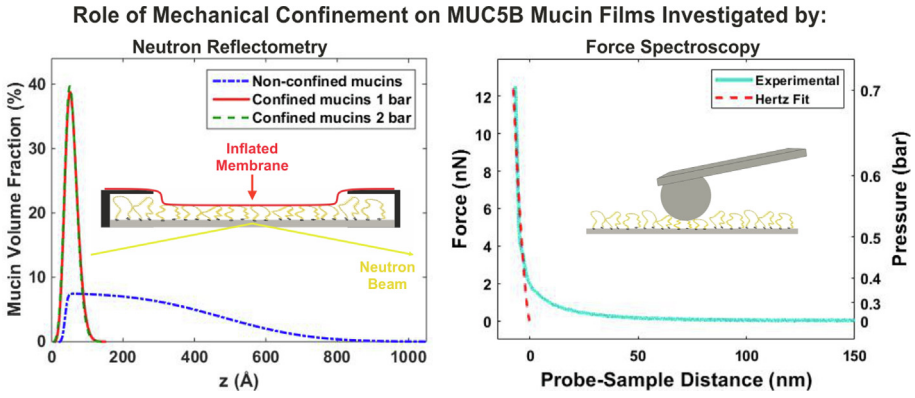

ARTICLE INFO

Article history:
Received 1 November 2021
Revised 5 January 2022
Accepted 16 January 2022
Available online 19 January 2022

Keywords:
Neutron reflectometry
Atomic force microscopy
Force spectroscopy

ABSTRACT

Hypothesis: Among other functions, mucins hydrate and protect biological interfaces from mechanical challenges. Mucins also attract interest as biocompatible coatings with excellent lubrication performance. Therefore, it is of high interest to understand the structural response of mucin films to mechanical challenges. We hypothesized that this could be done with Neutron Reflectometry using a novel sample environment where mechanical confinement is achieved by inflating a membrane against the films.
Experiments: Oral MUC5B mucin films were investigated by Force Microscopy/Spectroscopy and Neutron Reflectometry both at solid–liquid interfaces and under mechanical confinement.
Findings: NR indicated that MUC5B films were almost completely compressed and dehydrated when confined at 1 bar. This was supported by Force Microscopy/Spectroscopy investigations. Force Spectroscopy

Abbreviations: NR, Neutron Reflectometry; AFM, Atomic Force Microscopy; PBS, Phosphate Buffered Saline; SLD, Scattering Length Density; PS, Polystyrene; PEO, poly (ethylene oxide).

* Corresponding author at: Department of Biomedical Science, Malmö University, 20506 Malmö, Sweden.
E-mail address: javier.sotres@mau.se (J. Sotres).

[1] Both authors contributed equally to this work.

https://doi.org/10.1016/j.jcis.2022.01.096

Mechanical confinement
Mucins

also indicated that MUC5B films could withstand mechanical confinement by means of steric interactions for pressures lower than ~ 0.5 bar i.e., mucins could protect interfaces from mechanical challenges of this magnitude while keeping them hydrated. To investigate mucin films under these pressures by means of the employed sample environment for NR, further technological developments are needed. The most critical would be identifying or developing more flexible membranes that would still meet certain requirements like chemical homogeneity and very low roughness.

1. Introduction

Mucins, long glycoproteins with a central region that contains a high density of oligosaccharide side-chains (accounting for ca. 80% of their mass) [1], attract an enormous amount of research interest both because of their manifold role in biological systems and because of their multiple possibilities as biocompatible coatings. In living systems, mucins are the main component of mucus blankets [2] i.e., the viscous and hydrated gel that forms the outermost part of mucosal barriers. Mucus serves multiple purposes. It is a lubricious barrier that keeps mucosal surfaces hydrated and protects them from harsh chemical conditions, mechanical insults and pathogenic organisms [2,3]. Because of the difficulties associated with performing mucus studies, this component of mucosal barriers has been less investigated than the underlying mucosal layers. In this regard, *in vitro* physico-chemical studies of mucin and mucin-based films have significantly contributed to our understanding of these systems [4]. However, we still do not fully understand the mechanisms by which mucus fulfills many of its functions. For instance, little is known on the structure and hydration of mechanically challenged mucus.

Expecting a similar performance as that achieved in biological systems, mucins have also been investigated as coatings in biomedical applications. The performance of many medical implants and devices e.g., contact lenses, catheters, ventilation tubes, or stents is still challenged by unsatisfactory antibiofouling and tribological properties. The use of mucins as coatings on typically hydrophobic synthetic materials, which medicals devices are made from, has provided promising results. Mucin coatings not only efficiently suppress biofouling events, partially by conferring them with a hydrophilic character, but can also significantly reduce friction and wear [5–9]. However, in many cases passively adsorbed mucin coatings do not satisfactorily resist the mechanical stresses to which biomedical devices can be exposed. Subsequently, achieving stable resistant mucin-based coatings is attracting significant interest [10,11].

From the above discussion, it follows that understanding how the structure and hydration of mucin films change when mechanically confined would be of high interest not only for understanding how mucous films protect biological barriers, but also for the rational design of mucin-based coatings. The study of soft matter films under mechanical confinement was originally made possible by the emergence of the Surface Force Apparatus and the Atomic Force Microscope [12]. These techniques provide accurate interaction forces at different separations. Subsequently, they have been extensively used to study how mucus, mucins and mucin-based films respond to mechanical challenges [13–23]. However, they do not provide structural information. Indeed, going beyond measurements of forces and additionally measuring the near-surface structures has been a challenge for a number of decades. The main experimental difficulty has been to attain reproducible and accurate confinement within the restrictions of the analytical technique to be employed e.g., geometry, interference with the sensing probe, etc. The development by Cosgrove and collaborators of a confinement apparatus to be used in neutron reflectometry (NR) was a milestone in this direction [24–26]. Neutron reflectometry (NR) is indeed an ideal tool for extracting structural properties perpendicular to the surface of films under confinement, providing high resolution information on layer thickness, interface roughness, and layer density. In the mentioned setup, mechanical confinement was achieved by means of two quartz plates between which the sample was placed, and the pressure was controlled by a hydraulic ram. Since then, different variations of this mechanical confinement cell for NR studies have been proposed [27,28]. However, these setups suffered from some limitations such as the tendency of the plates to become misaligned, the long range waviness of the plates and the presence of entrained dust limiting the achievable confining separations. More recently, a setup with the potential to overcome these limitations was developed by de Vos *et al.* [29]. In this setup (Fig. 1), from now on referred as confinement cell, one of the rigid surfaces was replaced by a flexible membrane that can conform to long range waviness or bend around any entrained dust. This setup has been successfully used in a number of investigations on the structure of soft matter systems under confinement e.g., for poly-electrolyte multilayers [30,31], polymer brushes [32–34] and lipid bilayers [35].

The aim of this work was to test the potential of the presented mechanical confinement cell for NR studies to investigate the structure of mechanically confined mucin films. Specifically, films of the oral mucin MUC5B, one of the key components of salivary pellicles i.e., thin films formed upon selective adsorption of saliva that protect oral surfaces against chemical and mechanical insults [36].

2. Materials and methods

2.1. Chemicals

All water used was of ultrahigh quality (UHQ), processed in an Elgastat UHQ II apparatus (Elga Ltd., High Wycombe, Bucks, England). PBS buffer was prepared from tablets from Sigma Aldrich according to their instructions resulting in 137 mM NaCl, 2.7 mM KCl and 10 mM phosphate buffer solution (pH 7.4 at 25 °C). For neutron reflectivity experiments, deuterium oxide (D2O) of 99.9% atom% d was used (ref: 151882, Sigma-Aldrich, Germany). Dichlorodimethylsilane (≥99.5%, ref: 440272, Sigma-Aldrich, Germany), trichloroethylene (≥99.5%, ref: 251402, Sigma-Aldrich, Germany), ammonia (≥99.95%, ref: 09682, Sigma-Aldrich, Germany) and hydrogen peroxide solution (30 wt% in H2O, ref: 216763, Sigma-Aldrich, Germany) were also obtained from Sigma Aldrich. Polystyrene (MW: 62300 Da ref: ps22031) was purchased from PSS (Germany). Unless otherwise specified, all other chemicals used were of at least analytical grade.

2.2. Human salivary MUC5B

MUC5B was isolated from human whole saliva as previously described [37] using a modified version of the method described

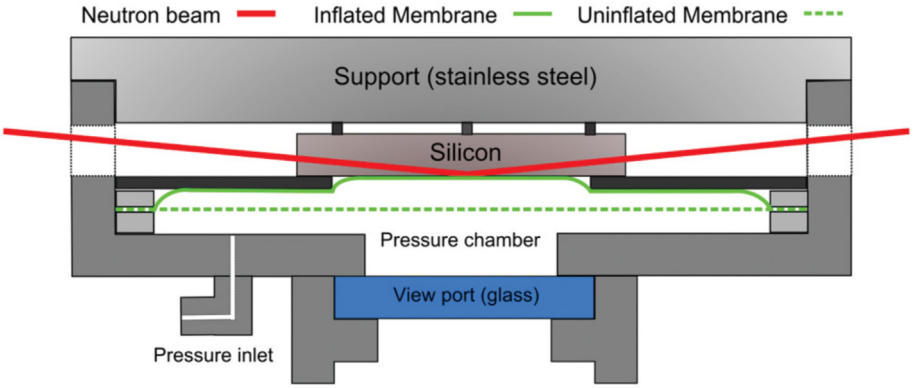

Fig. 1. Schematic diagram of the flexible-film confinement cell for NR studies [29]. A silicon block is placed on a stainless steel support, and exposed to solvent. A flexible membrane is then inflated by a known gas pressure, leading to the silicon and membrane surfaces coming into close contact. A masking ring on top of the silicon block (shown in dark grey) protects the membrane from overstretching. Reprinted from Review of Scientific Instruments, 2012, 83, 113903, with the permission of AIP Publishing.

in [38]. In short, whole saliva was mixed with an equal volume of 0.2 M NaCl followed by incubation overnight with stirring at 4 °C. After gentle centrifugation (4400 g for 30 min at 4 °C), the supernatant was subjected to density-gradient centrifugation in CsCl/0.1 M NaCl (Beckman Optima LE-80 K, rotor 50.2Ti, 36 000 r.p.m., 96 h, 15 °C, start density 1.45 g ml). Fractions were analyzed for density by weighing and measuring absorbance at 280 nm. MUC5B-containing fractions were identified using an antiserum, LUM5B-2, which recognizes the central domain of the MUC5B polypeptide backbone [39]. The MUC5B-containing fractions were pooled and dialysed against PBS (0.15 M NaCl, 5 mM NaHPO, pH 7) and then stored at −20 °C until used. MUC5B concentration was determined by extensive dialysis against water, freeze-drying and weighing, and estimated to be 0.3 $mg{\cdot}mL^{-1}$. Ethical approval was obtained from the committee of research ethics at Lund University (2018/42).

2.3. Cleaning and hydrophobization of silica substrates

Silica surfaces were used in all experiments. For force microscopy/spectroscopy, p-doped (boron) silicon wafers (Semiconductor Wafer Inc., Hsinchu, Taiwan) were used. For Neutron Reflectivity (NR) we used single crystal silicon (100) round blocks (diameter of 3 in.; polished by Sil'tronix Silicon Technologies, Archamps, France to a 5 Å RMS roughness). Surfaces were cleaned using a RCA protocol with 5:1:1 H_2O:NH_3:H_2O_2 at 80 °C for 10 min followed by additional 10 min of plasma cleaning in the case of AFM surfaces and UV/ozone cleaning in the case of NR surfaces. Regardless of the cleaning procedure, in all cases we obtained highly hydrophilic surfaces with water contact angles < 5°.

Subsequent hydrophobization of the silica surfaces was achieved by means of liquid-phase silanization [40]. Specifically, clean and dried silica surfaces were immersed in a solution containing 25 μL of dichlorodimethylsilane and 50 mL of trichloroethylene for one hour. After silanization, the surfaces were washed three times in trichloroethylene and three times in ethanol. The water contact angle after hydrophobization was ∼ 90°. The surfaces were stored in ethanol until use.

2.4. Neutron reflectometry (NR)

Neutron Reflectometry (NR) experiments were carried out at the D17 [41] reflectometer at the Institut Laue-Langevin, France (https://doi.org/10.5291/ILL-DATA.8–05-437; https://doi.org/10.5291/ILL-DATA.9–13-604; https://doi.org/10.5291/ILL-DATA.9–13-797) and at the INTER [42] reflectometer at ISIS, UK (https://doi.org/10.5286/ISIS.E.RB1810616; https://doi.org/10.5286/ISIS.E.RB1720422; https://doi.org/10.5286/ISIS.E.RB1610131), both time of flight reflectometers.

Initially, the hydrophobized substrates were clamped to a custom-made trough, specifically designed for investigating the round silicon blocks, in liquid media, used in this study. The trough is a machined silicon block (3 in. in diameter) with inlet and outlet holes to which PEEK tubes are glued. On the surface of the trough block there is a drilled circular groove (inner diameter 2.7 in., outer diameter 2.9 in.) into which a Viton O-ring is placed to provide space between the substrate and trough, as well as prevent leaks. The trough and substrate were clamped between two circular stainless steel plates, which were held together using stainless steel screws and bolts that pass through drilled holes. An image of the solid–liquid cell is provided in Supplementary Material Section S1. The silicon blocks mounted in this setup were initially characterized in PBS buffer prepared with both H_2O (hPBS, SLD = -0.56 × 10^{-6} $Å^{-2}$), and D_2O (dPBS, SLD = 6.36 × 10^{-6} $Å^{-2}$). Then, a 0.3 $mg{\cdot}ml^{-1}$ MUC5B in hPBS solution was flowed through the trough and left to adsorb for 1 h. The blocks were then extensively rinsed with dPBS and subsequently characterized once more in hPBS and dPBS. For experiments using this solid–liquid cell, incident angles of 0.4° and 2.8° were used at D17 and the δQ/Q resolution was 0.14. For the experiments at INTER, we used incident angles of 0.7° and 2.3°, and the δQ/Q resolution was 0.04.

Afterwards, the mucin-coated blocks were transferred from the solid–liquid cell to the NR confinement cell (Fig. 1), not allowing the coated side to dry at any moment. Full details for the experimental setup are provided in [29]. Briefly, the coated silicon blocks were mounted on a stainless steel support. The blocks were held in place by a stainless steel masking plate with an aperture in the center, exposing the mucin-coated silicon side. Attached to this mount is a pressure chamber with a flexible poly(ethylene terephthalate) (PET/Melinex®, DuPont-Teijin films) membrane on one of its faces. A masking plate provides support for the membrane when inflated and prevents it from overstretching and entering the beam path. The membrane is inflated against the silicon block by raising the internal pressure using a digital pressure regulator and a dry N_2 gas source. The masking ring contains two small holes (not shown in Fig. 1) that can be used for solvent to leave the cell. Under pressure, solvent can also easily leave the cell where the masking ring and the silicon block are in contact. At a pressure of ∼ 1 bar, the membrane and substrate were in good contact in a circular area of 35–45 mm in diameter. After a confining pressure was applied/incremented, the sample was always given at least 60 min to equilibrate. By doing short reflection experiments of only 10 min we could follow this equilibration process and only performed a full characterization if equilibrium was reached. After

the experiments, both samples and membranes were checked for damage. Overall, the samples did not show visual evidences of mechanical damage after the experiments. However, membranes did not recover their original shape. For this reason, samples were only investigated using increasing pressure ramps. For experiments using the NR confinement cell, incident angles of 0.4°, 1.2° and 2.8° were used at D17 and the δQ/Q resolution was 0.04. For experiments at INTER, we used incident angles of 0.3°, 0.7° and 2.3°, and the δQ/Q resolution was 0.04.

In our experiments, the Melinex was coated with a PS layer. This was achieved by spin coating 5 mL of a 10 g/L PS-toluene solution to the planar side of the Melinex while rotating it at 2000 rpm. The PS-coated Melinex was also characterized by means of AFM and NR. For NR characterization, PS-coated Melinex membranes were held under tension by a custom-made mechanical stretcher (Supplementary Material Section S2). This consists of two stainless steel rectangular blocks to which the edge of the Melinex can be secured by means of cylindrical stainless steel bars, held in place by adjustable springs. By maintaining tension using this set up, deformation of the membrane was avoided. For experiments using the mechanical stretcher, incident angles of 0.65° and 2.5° were used at D17 and the δQ/Q resolution was 0.04. For experiments at INTER, we used incident angles of 0.3°, 0.7° and 2.3°, and the δQ/Q resolution was 0.04.

NR Data Analysis: The measured reflected intensity, I(q), was normalized by the direct beam, I_0, to achieve the reflectivity, R (Q), where $Q = \frac{4\pi}{\lambda} sin(\theta)$, Q being the scattering vector, λ the neutron wavelength and θ the incident angle. R(Q) plots are provided as mean and standard deviation values of the reflectivities for a specific Q. Fitting of the R(Q) data was achieved using an optical matrix method [43] using the refnx software [44]. Specifically, the interface between the silicon support and the bulk solvent was considered as a stratified medium composed by different slabs. For error analysis of all NR data, we used the Bayesian Markov chain Monte Carlo (MCMC) approach implemented in the refnx software.

For fitting NR data from mechanically confined surfaces we used a mixed reflectivity model accounting for the fact that the overall interface comprised areas with different media in contact. In this approach, provided that the areas are not smaller than the relevant coherence length (∼10 μm), the overall reflectivity was considered a weighted average of the reflectivity from a type A contact (silicon/Melinex) and a type B contact accounting for the formation of pockets mainly filled with solvent when inflating the membrane (silicon/pockets) so that $R_{Total} = x \cdot R_A + (1 - x) \cdot R_B$ where $0 \leq x \leq 1$.

The parameters obtained by fitting NR data along with the SLD profiles were also used to approximate the Volume Fraction Profiles (VFP) of the different components of the interfaces using a modified version of the routine included in the refnx software for calculating SLD profiles as indicated in [45]. Briefly, this is done by initially setting the SLD for the component of interest to 1 and the SLD of all other components to 0. Then, recalculating the whole SLD profile using these SLD values along with all other parameters obtained previously from fitting the reflectivity curve results in the Volume Fraction Profile for the component of interest.

2.5. Atomic force microscopy and spectroscopy

A commercial Atomic Force Microscope (AFM) setup equipped with a liquid cell (MultiMode 8 SPM with a NanoScope V control unit, Bruker AXS, Santa Barbara CA) was used. For imaging experiments, we used triangular silicon nitride cantilevers with a nominal normal spring constant of 0.7 $N \cdot m^{-1}$ (ScanAsyst-Fluid, Bruker AFM Probes, Camarillo CA). For force spectroscopy experiments, we used rectangular silicon nitride cantilevers with a nominal normal spring constant of 0.76 $N \cdot m^{-1}$ (OMCL-RC800PSA, Olympus, Japan). AFM images were represented and analyzed with the WSxM software [46].

Scratching experiments were performed by scanning in contact mode an area of mucin films while applying a high load (∼100 nN). Then, a wider area was visualized by operating in the Peak Force Tapping Mode while applying a load of ∼ 1 nN.

Force ramps were acquired by using colloidal probes instead. For this, spherical silica particles with a nominal diameter of 15 μm (PSI-15.0, G. Kisker GbR, Germany) were attached to the free end of the cantilevers by using a two part epoxy adhesive (Loctite, Henkel Norden AB, Sweden). A micromanipulator (TransferMan NK 2, Eppendorf, Germany) was utilized to place glue, and subsequently the silica particle, on the free end of the cantilever. This was done with the help of an optical microscope (Nikon, Amsterdam, The Netherlands). Colloidal probes were visualized by variable pressure SEM (EVO LS10, Zeiss, Germany) for characterizing their shape and size. Force ramps (speed of 1 $\mu m \cdot s^{-1}$) were obtained at different lateral positions by operating the AFM in the force volume (FV) mode [47] and analyzed with the FSAS software (https://git.io/JmEOS). Analysis of force ramps was done following a process similar to that detailed in previous works [14,15,23]. Briefly, raw force ramps were first transformed into a deflection vs sample position representation by scaling the position sensitive photodetector signal by the slope of the contact region of force ramps obtained on a clean mica surface. Then, deflection was transformed into probe-sample interaction force by scaling the cantilever deflection by its spring constant, which was calculated for each cantilever by means of the thermal noise method [48]. Then, the region of the force ramp associated with mechanical contact was fitted with the Hertz contact model for a sphere-plane geometry. Extrapolating the Hertz fit to zero deflection provides the contact point i.e., the offset for the sample displacement values. The Hertz fit also allowed one to estimate the contact area for each cantilever deflection and, therefore, the pressure applied.

3. Results

3.1. Polystyrene-coated Melinex

The membrane to be used in the confinement cell, or at least the side in contact with the sample, needs to be characterized by a very low roughness (ideally below 1 nm) in order to achieve a smooth mechanical contact over large areas and to have a reasonable reflectivity, as this quantity decreases exponentially with increasing roughness. It is also beneficial if the membranes are characterized by a Scattering Length Density (SLD) higher than that of the sample support, typically silicon (SLD = 2.07×10^{-6} $Å^{-2}$). This will result in the presence of a critical angle, which will confirm whether confinement is achieved when applying a pressure. Following previous works [29–33], we used a 50 μm thick poly(ethylene terephthalate) (PET) film, traded under the name Melinex®, which meets these characteristics. Melinex can be acquired from DuPont Teijin films Ltd. without going through the roughing process that most films for commercial use are subjected to. This results in a film with one of its sides with a roughness in the ∼ nm order. However, AFM imaging revealed that that this planar side was also easily contaminated and could not be satisfactorily cleaned with standard protocols e.g., water/ethanol/water washing steps followed by N_2 drying (features with sizes in the 10–200 nm range could still be observed after cleaning as shown in Supplementary Material Section S3). In order to make sure that the membrane was completely cleaned (critical for NR experi-

ments, as it was not possible to characterize it with AFM just before), plasma or ozone/UV cleaning was required. However, this step increased Melinex roughness, ending up with a RMS roughness for its planar side of ∼ 3 nm (Supplementary Material Section S3).

In order to achieve a lower roughness while keeping the flexible membrane clean from contaminants features, just after ozone/UV cleaning we spin-coated the Melinex with polystyrene (PS). As shown by AFM imaging (Fig. 2a), this resulted in a RMS roughness for its topography of ∼ 3 Å. In order to characterize the thickness of the PS-coating as well as to experimentally determine the SLD of the Melinex (required for modelling NR data from mechanical contact experiments), NR was used to characterize the PS-coated Melinex in air. NR raw and fitted data is provided in Fig. 2b. The corresponding SLD profile is provided in Fig. 2c. The values for all fitting parameters are provided in Supplementary Material Section S4. Overall, NR indicated a thickness for the PS coating of 33 ± 2 Å and a SLD for the Melinex of $(2.53 \pm 0.01) \times 10^{-6}$ Å^{-2}.

3.2. NR of non-confined mucin films

Films of MUC5B mucins were formed by flowing a 0.3 mg·ml^{-1} MUC5B in hPBS solution through the NR solid–liquid cell containing the hydrophobized silica/silicon blocks. Previous studies showed that MUC5B mucins rapidly and irreversibly adsorb to hydrophobized silica surfaces [14] and at the investigated bulk concentration values the surface adsorbed amount has already achieved a close to maximum value i.e., the surface amount barely increases if higher bulk concentrations are used [49].

Before mechanical confinement experiments, we always characterized by means of NR the mucin-coated hydrophobized silicon blocks in the NR solid–liquid cell after rinsing with mucin-free PBS buffer. Representative experiments, fitted to a Si/SiO_2/Silanes/Mucins/Solvent model and corresponding SLD profiles in both hydrogenated and deuterated PBS buffer are shown in Fig. 3.

Relevant fit parameters are provided in Table 1 (values for all fitting parameters are provided in Supplementary Material Section S5). It can be observed that mucin films extended up to ∼ 440 Å from the surface, being highly hydrated (∼92%, in good agreement with previous reports [4]) and exhibited a high tendency for deuteration, as indicated by their different SLD values in hydrogenated and deuterated buffer solutions (Supplementary Material Section S5), in good agreement with previous reports [50].

3.3. NR of mechanically confined mucin films

NR data obtained while mechanically confining the MUC5B mucin films at both 1 and 2 bar is presented in Fig. 4a. A clear critical angle was observed at Q ∼ 0.0049 Å^{-1} for both investigated pressures. The location of this critical angle is what is expected for a silicon/Melinex interface (provided a SLD of 2.53·10^{-6} Å^{-2} found from the fit in Fig. 2). Hence, this clearly shows that most dPBS was expelled and that the silicon and the Melinex could be brought into close proximity. The NR curve obtained at 1 bar shows also another clear feature at Q ∼ 0.012 Å^{-1}. This was unlikely due to a layer of dPBS trapped between the silicon and Melinex as secondary fringes were not observed. Instead, it was more likely due to a small contribution of a reflection from a different interface. This additional feature/peak was also observed in previous experiments with the employed confinement cell e.g., [29], and was associated with the presence of pockets where complete mechanical confinement was not achieved, therefore, containing trapped (deuterated in this particular case) solvent. This hypothesis was supported by the fact that the mentioned feature was less pronounced after incrementing the pressure from 1 bar to 2 bar so that the solvent trapped in these pockets was eventually squeezed

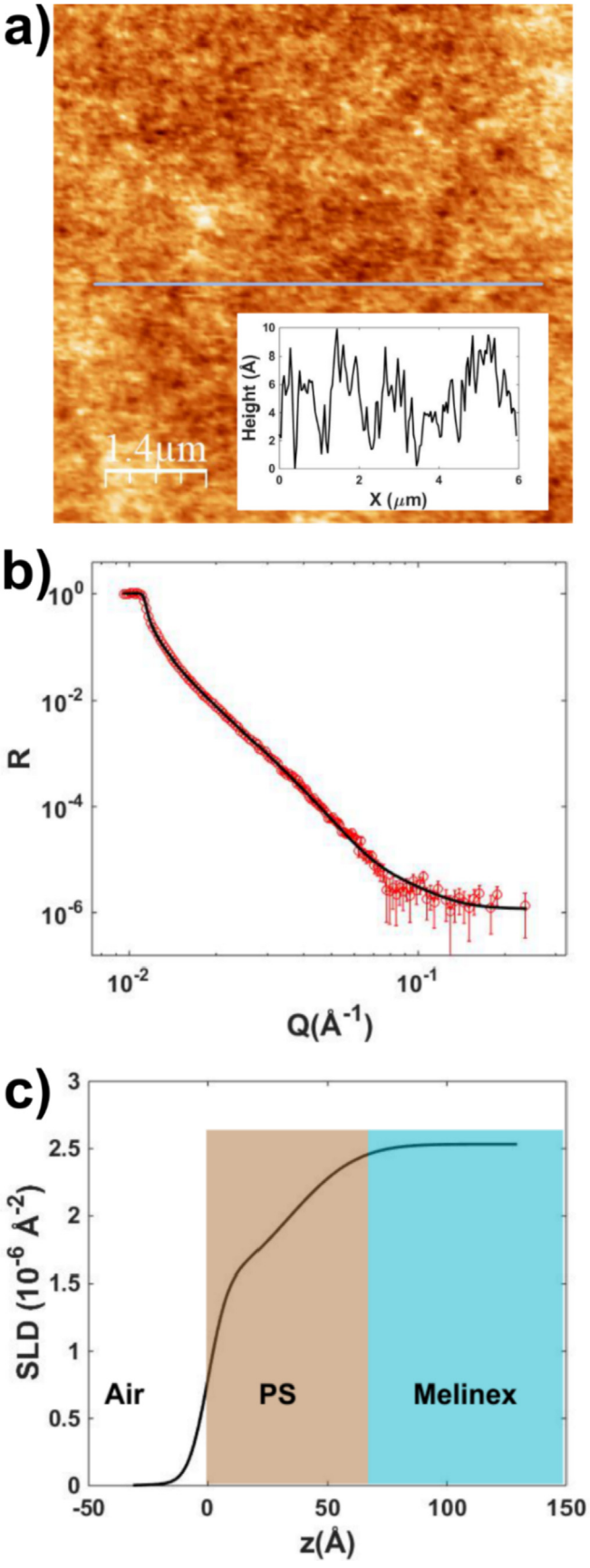

Fig. 2. a) AFM image of a PS-coated Melinex surface. The inset shows the height profile along the highlighted line. **b)** Fitted NR data and **c)** SLD profile for the PS-coated Melinex in air.

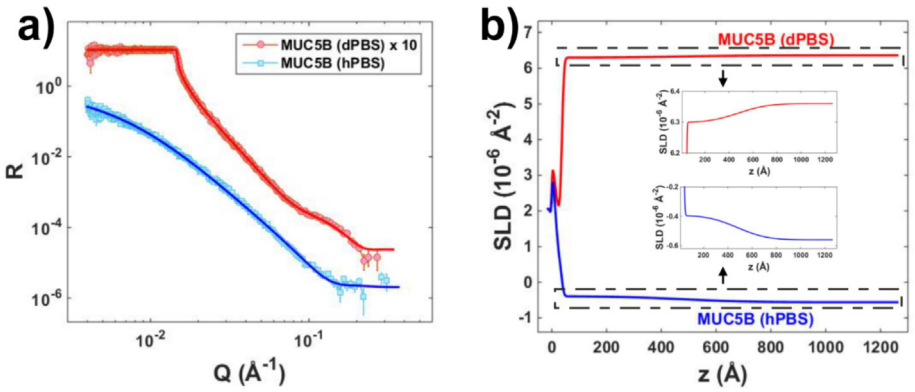

Fig. 3. a) Fitted NR data and **b)** corresponding SLD profiles for a MUC5B mucin coated hydrophobized silicon block in both dPBS and hPBS solvents.

Table 1
Thickness and hydration values obtained by fitting NR data for the non-confined mucin films as well as for the mucin films mechanically confined (*Reflectivity A*) at 1 and 2 bar.

	Thickness (Å)	Hydration (%)
MUC5B 0 bar (non-confined)	440.0 ± 70.0	92 ± 1
MUC5B 1 bar	23.9 ± 1.6	31 ± 6
MUC5B 2 bar	22.1 ± 1.2	25 ± 4

away. Therefore, for fitting NR data obtained under mechanical confinement we used a mixed reflectivity model, as indicated in the Materials and Methods section, accounting for the reflection from:

- *Reflectivity A*: Si/SiO_2/Silanes/Mucins/PS/Melinex interface.
- *Reflectivity B*: Si/SiO_2/Silanes/Mucins/Pockets interface (accounting for the areas where the Melinex was kept away from the silicon).

An illustration for these hypothesized structures is provided in Fig. 4b. As shown in Fig. 4a, this model provided a good fit for the experimental data, supporting our hypothesis. The contribution from the pockets i.e., *Reflectivity B*, decreased from 1.3% at 1 bar to 0.4% at 2 bar (Supplementary Material Section S6). This indicates that the solvent trapped in the pockets was squeezed away when incrementing the pressure. SLD profiles for *Reflectivity A* i.e., for the areas where the mucins were mechanically confined, at both 1 and 2 bar are shown in Fig. 4c. For comparison, Fig. 4d shows the Volume Fraction Profiles obtained for the mucin layer from the SLD profile of *Reflectivity A* i.e., for the mechanically confined mucins, along with the Volume Fraction Profile obtained from the respective SLD profiles for the non-confined mucins (Fig. 3b). Thickness and hydration values used for fitting the non-confined mucins, and for the mucin layers confined at 1 and 2 bar are shown in Table 1 (values for all fitting parameters, as well as the SLD profiles for *Reflectivity B*, are provided in the Supplementary Material Section S6).

Overall, the NR data for the mucin films confined at 1 bar could be fitted with a thickness and hydration for the films of $\sim$ 2 nm and $\sim$ 30% respectively, in contrast with the $\sim$ 44 nm thickness and the $\sim$ 90% hydration for the non-confined films. Increasing the confining pressure to 2 bar had barely an effect on the thickness and hydration that resulted from fitting the NR data to a similar model. Further insight can be obtained from the Volume Fraction profile. By integrating this profile (in terms of relative fraction rather than %) along the surface normal direction, it is possible to obtain the mucin volume per unit surface area. For the non-confined mucin films this results in $\sim$ 33 Å whereas for the confined mucins at both investigated pressures a value of $\sim$ 17 Å is obtained. This indicates that mechanical confinement not only resulted in solvent being expelled but also in some mucins being removed from the confined region.

3.4. Thickness of mechanically confined MUC5B mucin films determined from AFM scratching experiments

In order to validate NR data, the thickness of mechanically confined MUC5B films was also measured by AFM. For this, areas of freshly prepared films were scratched with the AFM tip by operating the AFM in the contact mode at high loads ($\sim$100 nN). Subsequently, the scratched areas were visualized at lower loads ($\sim$1 nN) while operating the AFM in the Peak Force Tapping mode minimizing, therefore, the destructive lateral forces. Both scratching and imaging procedures were performed with PBS buffer as the ambient medium. Results from a representative scratch are shown in Fig. 5. It can be seen that the thickness obtained in these experiments, 2–3 nm, is in good agreement with the thickness provided by NR for mechanically confined MUC5B films. Incrementing the load did not lead to lower thickness values, but to dragging of mucins along the scratched area instead. The exerted pressure during AFM imaging was most probably higher than that applied in NR experiments. Specifically, while the mechanical pressure applied on the films during AFM imaging cannot be accurately estimated because of the uncertainty in the contact area, it is still possible to make a rough estimation. For an applied load of $\sim$ 1 nN and a contact area of $\sim$ 100 nm^2, the applied pressure would be $\sim 10^2$ bar, a higher value than that applied with the confinement cell in our NR experiments.

3.5. Force spectroscopy on MUC5B mucin films

To further understand our NR data on confined MUC5B mucin films, we investigated this system by means of AFM-based force spectroscopy. AFM force ramps provide accurate measurements acting on the AFM probe at different relative positions from a sample. When in mechanical contact, several models are available for describing the interaction between probe and sample. Among those, we have used the Hertz model. The choice was based on the fact that adhesions were almost non-existent in our experiments. We used this approach as mechanical contact models do not only describe the force vs sample indentation behavior, but also provide an estimation of the contact area at different forces. Thus, fitting force ramps will also allow the estimation of pressure values that can be compared to those applied in NR experiments. However, this approach requires a probe with a well-defined geometry. Subsequently, we used colloidal probes with an average

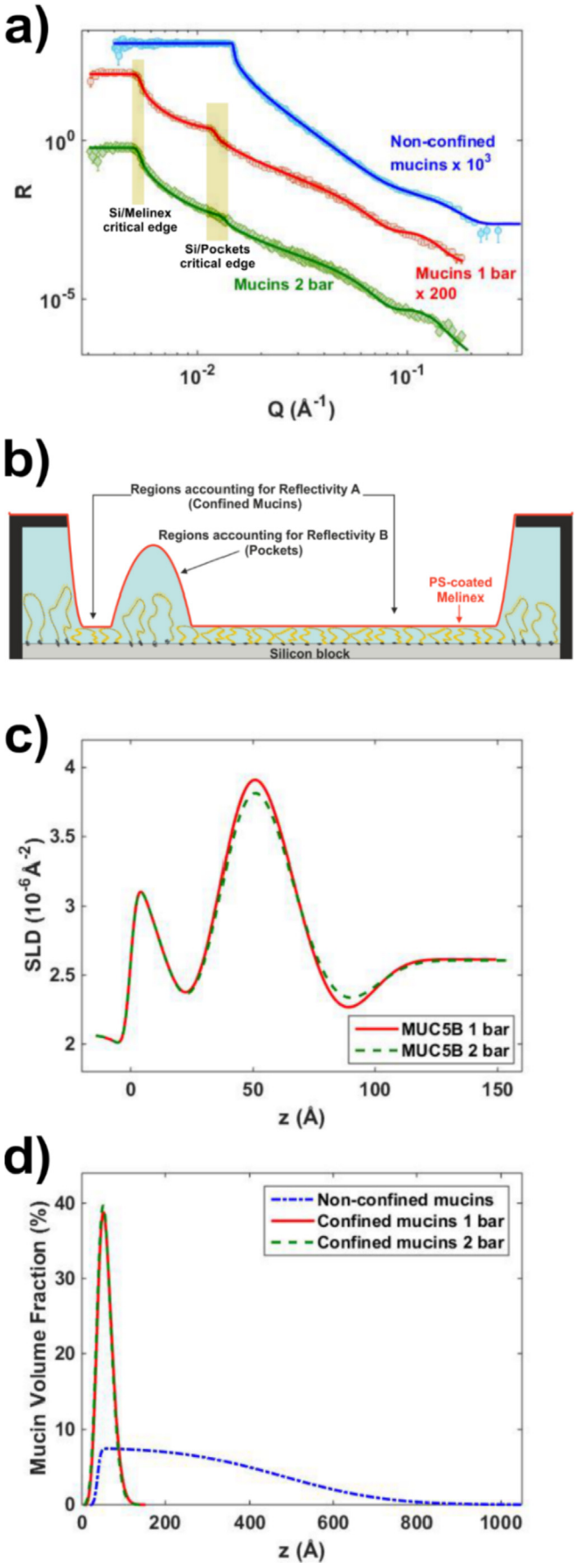

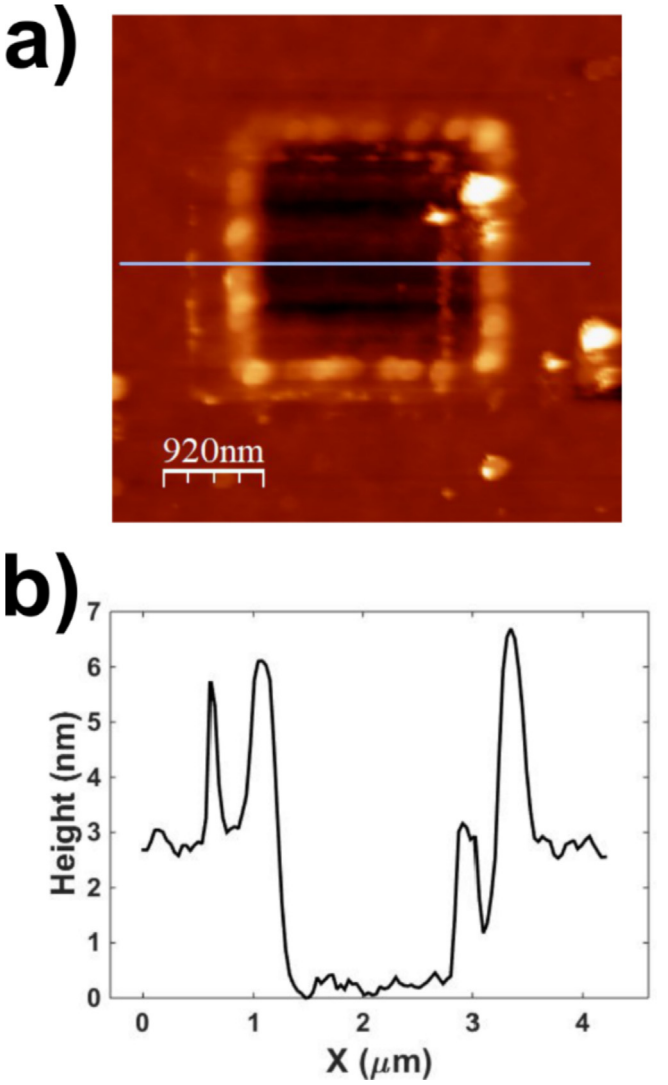

Fig. 5. a) AFM topography image of a scratched mucin film and **b)** height profile along the highlighted line in the topography image.

diameter of 15 μm (according to the manufacturer). Nevertheless, we always characterized the probes by means of SEM imaging before use in order to have an accurate estimation of the radius of each probe (Fig. 6a). Fig. 6b shows a force vs. probe sample ramp (solid line) representative from these experiments. Two regimes are clearly differentiated at short separations. Initially, the force exhibits an exponential dependence with the separation, previously reported for force ramps on mucin films [14] and representative of a steric repulsion. At shorter separations, forces exhibit a dependence with separation that is well fitted (dashed line in Fig. 6b) by the Hertz contact model:

Fig. 4. a) NR data obtained while mechanically confining the MUC5B mucin films in dPBS at both 1 and 2 bar. Critical edges for the Si/Melinex and the Si/"pockets" interfaces are highlighted. NR data for the non-confined mucin films in dPBS is included for comparison. **b)** Illustration for the situation under an applied pressure, where regions of mechanically confined mucins (*Reflectivity A*) coexist with regions with pockets (*Reflectivity B*). **c)** Corresponding SLD profiles for the films confined at 1 and 2 bar (*Reflectivity A*). **c)** Volume fraction profiles for the non-confined and confined mucin films derived from the SLD profiles.

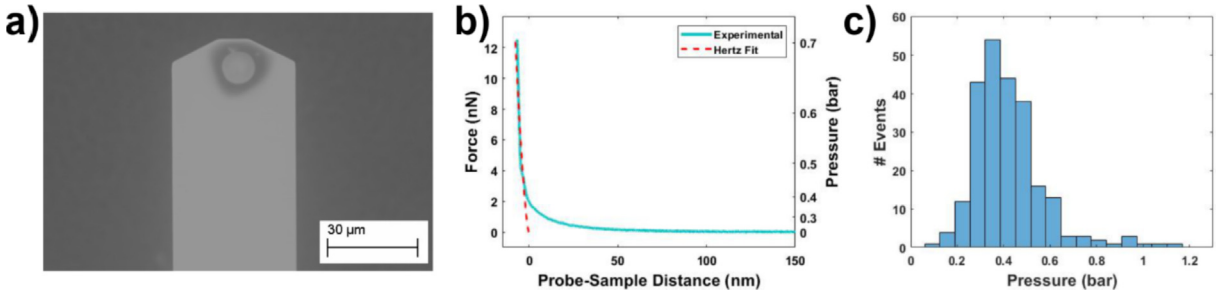

Fig. 6. **a)** SEM image of a colloidal probe used in our experiments. **b)** Force vs. probe sample distance ramp on a mucin film obtained with a colloidal probe (solid line) and fit to the Hertz contact model (dashed line). The right vertical axis indicate the pressures corresponding to the forces of the Hertz fit. **c)** Histogram of the pressures, according to the Hertz model, for which the force ramps entered the region defined by the Hertz model.

$$F_{Hertz}(\delta) = \frac{4ER^{1/2}}{3(1-\upsilon^2)}\delta^{3/2}$$

where E is the Young's modulus of the sample, R is the radius of the probe, ν the Poisson ratio of the sample and δ is the deformation of the sample [51]. Though, deviations from the Hertz model occurred at high forces, which is not unexpected as the applicability of the Hertz model is based on the assumption than the thickness of the film is lower than the radius of the probe. Nevertheless, the use of the Hertz model still allowed to estimate the pressures exerted by the probe when in mechanical contact. Specifically, in the Hertz model, the contact radius, r_c, can be estimated by $r_c = \sqrt{\delta R}$ where δ is the indentation/deformation. Thus, the pressure, P, can be estimated as $P = F/\pi r_c^2$. In the right vertical axis of Fig. 6b the pressures corresponding to the Hertz fit are shown. In this example, it can be seen that the pressure for which the force entered the regime described by the Hertz model is well-below 1 bar. Fig. 6c shows a histogram, calculated from 256 force ramps, of the pressures for which the force ramp entered the Hertz mechanical contact regime. Again, this shows that for the vast majority of measurements this threshold value was well below 1 bar i.e., the minimum pressure for which we were able to perform NR confinement experiments. We can also see from Fig. 6b that the indentation of the sample after the curves entered the Hertz regime barely increased with force/pressure, even less than that predicted by the Hertz model, which is expected providing that the thickness of the film was significantly smaller, according to our NR data, than the probe size.

4. Discussion

NR experiments performed with the confinement cell showed that, when confined at 1 bar, the MUC5B mucin films were almost completely compressed and dehydrated. Specifically, the film thickness and hydration parameters in the models used to fit the NR data decreased from ∼ 440 Å to ∼ 24 Å and from ∼ 92% to ∼ 31% respectively. The values of these parameters barely changed when fitting the NR data obtained for the films confined at 2 bar. Interestingly, the value of the thickness parameter obtained after fitting the NR data of the mechanically confined films were in good agreement with the ∼ 2–3 nm thickness provided by AFM imaging of scratched areas of the films. As discussed above, the mechanical pressure applied on the films during AFM imaging was in the order of ∼ 10^2 bar. This is a higher value than that applied with the confinement cell in our NR experiments so that the thickness provided by AFM also corresponds to that of fully compressed mucin films.

In order to estimate the pressures that would originate relevant changes in e.g., the thickness and hydration of the mucin films, colloidal probe force spectroscopy experiments were performed. In good agreement with previous results, force ramps performed on these systems exhibited two differentiated regimes when approaching probe and sample: an initial repulsive regime with an exponential-like dependence with separation, characteristic of steric repulsions, followed by a regime where the force exhibited a steeper dependence with the separation that could be well fitted by the Hertz contact model. Fitting to the contact model combined with the knowledge of the size and geometry of the probe allowed to estimate the relationship between applied pressure and deformation. Specifically, we found that for the vast majority of performed force ramps, for a pressure of 1 bar i.e., the minimum value at which we were able to operate the NR confinement cell, mechanical contact was already established, and above this value deformation barely increased with applied pressure. From this data, it could also be inferred that the pressures for which the probe and sample interact by means of steric repulsion typically lay below 0.5 bar. This would be the pressures for which mucin films could protect interfaces from mechanical challenges while keeping them highly hydrated. It would be interesting to investigate the films at these pressures by means of the NR confinement cell, not only because then significant structural changes with pressure would be observed but also because of its relevance for *in vivo* situations. For example, pressures applied during tongue and labial movements have been reported to be in the order of ∼ 0.1 bar [52,53]. Nevertheless, the pressures that can be achieved with the current setup can be of relevance for some other situations. For example, teeth, which are covered by a thin layer of salivary components including MUC5B in the outer surface of this layer [14,54], can be exposed to biting pressures in the order of ∼ 10 bar [55,56]. Our work indicates that under these pressures, the outer layer of teeth pellicle, and probably the whole pellicle considering that the inner layer is composed mainly of small globular proteins, will be almost completely compressed and dehydrated.

We only studied MUC5B mucin films formed by adsorption from 0.3 mg·mL^{-1} bulk solutions. It is reasonable to expect that structural changes induced by confinement will depend on the surface concentration of mucins. However, 0.3 mg·mL^{-1} was the highest concentration obtained during purification, and increasing the concentration would have required procedures that could irreversibly damage the mucins. Nevertheless, previous studies showed that the surface amount of MUC5B mucins had already a weak dependence with bulk concentration at these values [49]. Thus, it is unlikely that different results than those reported would have been obtained by investigating films formed from bulk solutions of higher mucin concentrations.

As mentioned, the minimum pressure that we could apply during a NR experiment with the confinement cell was ∼ 1 bar. This originated from the requirement that the area confined by the

membrane needs to be bigger than the area illuminated by the neutron beam (~1–10 cm^2). Thus, the minimum pressure that can be applied during an experiment is that for which the membrane is deformed enough to achieve a mechanical contact area with the sample of ~ 1–10 cm^2. This is determined by the flexibility of the membrane. However, flexibility is not the only characteristic that the membrane needs to fulfill. The membrane, or at least the side in contact with the sample, needs to be characterized by a very low roughness (ideally below 1 nm) in order to achieve a smooth mechanical contact over large areas and to have a reasonable reflectivity, as this quantity decreases exponentially with increasing roughness. The membrane needs to be characterized as well by a homogeneous chemical composition. If μm-sized domains of different chemical composition are present, the resulting data will be a combination of different reflectivities. This would enormously increase the complexity of the analysis of the data, to an extent where obtaining reliable information would be almost impossible. Moreover, in these experiments, where studies at different contrasts are impractical because of the impossibility to change the solvent once mechanical contact is established, a reliable analysis of the data is highly dependent on the presence of a critical angle. For this to happen, the membrane needs to be characterized by a SLD higher than that of the sample support, typically silicon (SLD = $2.07 \times 10^{-6} Å^{-2}$). These characteristics are fulfilled by Melinex, which has been so far the membrane used in all reported experiments performed with the confinement cell [29–34]. However, for the minimum pressure we were able to operate using Melinex as a membrane i.e., 1 bar, the MUC5B mucin films were fully compressed. This was also observed e.g., for uncharged polymer brushes when investigated with the confinement cell [32]. This suggests that for studying these type of soft matter systems by means of the confinement cell for NR studies, one would need to identify and use different membranes, more flexible than Melinex so that a wide area in mechanical contact could be establish for pressures well below 0.5 bar (as indicated by our force spectroscopy experiments), but that would still fulfill all the characteristics indicated above.

5. Conclusions

The goal of this work was to investigate the potential of a recently developed confinement cell for studying by means of NR the structure of MUC5B mucin films under mechanical confinement. In this setup, by inflating a Melinex membrane against mucin films we were able to establish mechanical confinement at a pressure of 1 bar. Overall, NR indicated that at this pressure the mechanically confined mucin films were already almost completely compressed and dehydrated. While increasing the pressure to 2 bar increased the sample area mechanically confined by the membrane, this had almost no effect on the structure of the already mechanically confined mucins. We also used AFM to validate NR results. Specifically, AFM investigations provided a thickness for the fully compressed mucin films of 2–3 nm, which was in good agreement with the film thickness parameter used to fit NR data. AFM also confirmed that for a pressure of 1 bar the interaction between AFM probes and mucin films could be described by a mechanical contact model, where the deformation of the films barely changed with applied pressure. Thus, AFM experiments proved the validity of our analysis of NR data. While several previous works have investigated how mucin films oppose mechanical load e.g., [14,19,21,22], this is the first work that provides insight on how this affects the structure and hydration of these films.

We have also identified key improvements of the NR confinement cell from which structural studies of thin soft matter films would benefit. As indicated by the presented AFM force spectroscopy experiments, for investigating the mucin films in a regime where steric repulsion could withstand the mechanical pressure exerted by the membrane in NR experiments it would be needed to achieve a good mechanical contact at pressures of 0.5 bar and below. This would be the pressure range where mucin films would be able to provide mechanical protection to interfaces while keeping them hydrated. Going below the current 1 bar limit would benefit the study of other systems as well. For example, full compression at 1 bar was also reported for PEO polymer brushes when investigated with the confinement cell [32]. As we discussed, for this it will be necessary to identify or develop membranes more flexible than Melinex but that still would meet certain requirements like very low roughness and chemical homogeneity.

CRediT authorship contribution statement

Juan F. Gonzalez-Martinez: Methodology, Investigation, Formal analysis, Writing – original draft, Writing – review & editing. **Hannah Boyd:** Methodology, Investigation, Formal analysis, Writing – original draft, Writing – review & editing. **Philipp Gutfreund:** Investigation, Formal analysis, Writing – review & editing. **Rebecca J.L. Welbourn:** Investigation, Writing – review & editing. **Carolina Robertsson:** Methodology, Investigation, Writing – review & editing. **Claes Wickström:** Methodology, Investigation, Writing – review & editing. **Thomas Arnebrant:** Conceptualization, Writing – review & editing, Funding acquisition. **Robert M. Richardson:** Methodology, Investigation, Writing – review & editing. **Stuart W. Prescott:** Methodology, Investigation, Writing – review & editing. **Robert Barker:** Conceptualization, Methodology, Investigation, Writing – review & editing, Funding acquisition. **Javier Sotres:** Conceptualization, Methodology, Software, Writing – original draft, Writing – review & editing, Funding acquisition.

Declaration of Competing Interest

The authors declare that they have no known competing financial interests or personal relationships that could have appeared to influence the work reported in this paper.

Acknowledgments

The Swedish Research Council (Grant No. 2016-06950), Nordforsk (Grant No. 87794), the Knowledge Foundation (Grant No. 20190010), the Gustav Th. Ohlsson Foundation and Malmö University are acknowledged for financial support. R.B. would like to acknowledge the support of the Royal Society Industrial Fellowship (Grant No. SIF\R1\181005) and the Engineering and Physical Sciences Research Council in the UK (Grant No. EP/R022534/1).

Appendix A. Supplementary data

Supplementary data to this article can be found online at https://doi.org/10.1016/j.jcis.2022.01.096.

References

[1] J. Dekker et al., The MUC family: an obituary, Trends Biochem. Sci. 27 (3) (2002) 126–131.
[2] M.E. Johansson, H. Sjövall, G.C. Hansson, The gastrointestinal mucus system in health and disease, Nat. Rev. Gastroenterol. Hepatol. 10 (6) (2013) 352–361.
[3] R.A. Cone, Barrier properties of mucus, Adv. Drug Deliv. Rev. 61 (2) (2009) 75–85.
[4] O. Svensson, T. Arnebrant, Mucin layers and multilayers — Physicochemical properties and applications, Curr. Opin. Colloid Interface Sci. 15 (6) (2010) 395–405.
[5] J.B. Madsen, J. Sotres, K.I. Pakkanen, P. Efler, B. Svensson, M. Abou Hachem, T. Arnebrant, S. Lee, Structural and Mechanical Properties of Thin Films of Bovine

Submaxillary Mucin versus Porcine Gastric Mucin on a Hydrophobic Surface in Aqueous Solutions, Langmuir 32 (38) (2016) 9687–9696.
[6] G. Petrou, T. Crouzier, Mucins as multifunctional building blocks of biomaterials, Biomater. Sci. 6 (9) (2018) 2282–2297.
[7] C.A. Rickert et al., Highly Transparent Covalent Mucin Coatings Improve the Wettability and Tribology of Hydrophobic Contact Lenses, ACS Appl. Mater. Interfaces 12 (25) (2020) 28024–28033.
[8] L. Shi et al., Mucin coating on polymeric material surfaces to suppress bacterial adhesion, Colloids Surf. B 17 (4) (2000) 229–239.
[9] J. Sotres, J.B. Madsen, T. Arnebrant, S. Lee, Adsorption and nanowear properties of bovine submaxillary mucin films on solid surfaces: Influence of solution pH and substrate hydrophobicity, J. Colloid Interface Sci. 428 (2014) 242–250.
[10] J. Song, T.M. Lutz, N. Lang, O. Lieleg, Bioinspired Dopamine/Mucin Coatings Provide Lubricity, Wear Protection, and Cell-Repellent Properties for Medical Applications, Adv. Healthcare Mater. 10 (4) (2021) 2000831, https://doi.org/10.1002/adhm.v10.4.
[11] B. Winkeljann, M.G. Bauer, M. Marczynski, T. Rauh, S.A. Sieber, O. Lieleg, Covalent Mucin Coatings Form Stable Anti-Biofouling Layers on a Broad Range of Medical Polymer Materials, Adv. Mater. Interfaces 7 (4) (2020) 1902069, https://doi.org/10.1002/admi.v7.4.
[12] J. Sotres, T. Arnebrant, Experimental Investigations of Biological Lubrication at the Nanoscale: The Cases of Synovial Joints and the Oral Cavity, Lubricants 1 (4) (2013) 102–131.
[13] J. An, C. Jin, A. Dėdinaitė, J. Holgersson, N.G. Karlsson, P.M. Claesson, Influence of Glycosylation on Interfacial Properties of Recombinant Mucins: Adsorption, Surface Forces, and Friction, Langmuir 33 (18) (2017) 4386–4395.
[14] H. Boyd, J.F. Gonzalez-Martinez, R.J.L. Welbourn, P. Gutfreund, A. Klechikov, C. Robertsson, C. Wickström, T. Arnebrant, R. Barker, J. Sotres, A comparison between the structures of reconstituted salivary pellicles and oral mucin (MUC5B) films, J. Colloid Interface Sci. 584 (2021) 660–668.
[15] H. Boyd, J.F. Gonzalez-Martinez, R.J.L. Welbourn, K. Ma, P. Li, P. Gutfreund, A. Klechikov, T. Arnebrant, R. Barker, J. Sotres, Effect of nonionic and amphoteric surfactants on salivary pellicles reconstituted in vitro, Sci. Rep. 11 (1) (2021), https://doi.org/10.1038/s41598-021-92505-4.
[16] M. Cárdenas, J.J. Valle-Delgado, J. Hamit, M.W. Rutland, T. Arnebrant, Interactions of Hydroxyapatite Surfaces: Conditioning Films of Human Whole Saliva, Langmuir 24 (14) (2008) 7262–7268.
[17] I.C. Hahn Berg, L. Lindh, T. Arnebrant, Intraoral Lubrication of PRP-1, Statherin and Mucin as Studied by AFM, Biofouling 20 (1) (2004) 65–70.
[18] I.C. Hahn Berg, M.W. Rutland, T. Arnebrant, Lubricating Properties of the Initial Salivary Pellicle — an AFM Study, Biofouling 19 (6) (2003) 365–369.
[19] M. Malmsten, E. Blomberg, P. Claesson, I. Carlstedt, I. Ljusegren, Mucin layers on hydrophobic surfaces studied with ellipsometry and surface force measurements, J. Colloid Interface Sci. 151 (2) (1992) 579–590.
[20] T. Nylander, T. Arnebrant, P.-O. Glantz, Interactions between salivary films adsorbed on mica surfaces, Colloids Surf. A Physicochem. Eng. Asp. 129-130 (1997) 339–344.
[21] E. Perez, J.E. Proust, Forces between mica surfaces covered with adsorbed mucin across aqueous solution, J. Colloid Interface Sci. 118 (1) (1987) 182–191.
[22] T. Pettersson, A. Dėdinaitė, Normal and friction forces between mucin and mucin-chitosan layers in absence and presence of SDS, J. Colloid Interface Sci. 324 (1-2) (2008) 246–256.
[23] J. Sotres, S. Jankovskaja, K. Wannerberger, T. Arnebrant, Ex-Vivo Force Spectroscopy of Intestinal Mucosa Reveals the Mechanical Properties of Mucus Blankets, Sci. Rep. 7 (1) (2017), https://doi.org/10.1038/s41598-017-07552-7.
[24] T. Cosgrove et al., The measurement of volume fraction profiles for adsorbed polymers under compression using neutron reflectometry, Colloids Surf. A Physicochem. Eng. Asp. 86 (1994) 103–110.
[25] T. Cosgrove et al., Surface force and neutron scattering studies on adsorbed poly(2-vinylpyridine)-b-polystyrene, Colloids Surf. A Physicochem. Eng. Asp. 86 (1994) 91–101.
[26] T. Cosgrove, A. Zarbakhsh, P.F. Luckham, M.L. Hair, J.R.P.W. Webster, Adsorption of polystyrene–poly(ethylene oxide) block copolymers on quartz using a parallel-plate surface-force apparatus and simultaneous neutron reflection, Faraday Discuss. 98 (1994) 189–201.
[27] T.L. Kuhl, G.S. Smith, J.N. Israelachvili, J. Majewski, W. Hamilton, Neutron confinement cell for investigating complex fluids, Rev. Sci. Instrum. 72 (3) (2001) 1715, https://doi.org/10.1063/1.1347981.
[28] J.-H. Cho, G.S. Smith, W.A. Hamilton, D.J. Mulder, T.L. Kuhl, J. Mays, Surface force confinement cell for neutron reflectometry studies of complex fluids under nanoconfinement, Rev. Sci. Instrum. 79 (10) (2008) 103908, https://doi.org/10.1063/1.3005483.
[29] W.M. de Vos, L.L.E. Mears, R.M. Richardson, T. Cosgrove, R.M. Dalgliesh, S.W. Prescott, Measuring the structure of thin soft matter films under confinement: A surface-force type apparatus for neutron reflection, based on a flexible membrane approach, Rev. Sci. Instrum. 83 (11) (2012) 113903, https://doi.org/10.1063/1.4767238.
[30] W.M. de Vos, L.L.E. Mears, R.M. Richardson, T. Cosgrove, R. Barker, S.W. Prescott, Nonuniform Hydration and Odd-Even Effects in Polyelectrolyte Multilayers under a Confining Pressure, Macromolecules 46 (3) (2013) 1027–1034.
[31] S.B. Abbott, W.M. de Vos, L.L.E. Mears, R. Barker, R.M. Richardson, S.W. Prescott, Hydration of Odd-Even Terminated Polyelectrolyte Multilayers under Mechanical Confinement, Macromolecules 47 (10) (2014) 3263–3273.
[32] S.B. Abbott et al., Is Osmotic Pressure Relevant in the Mechanical Confinement of a Polymer Brush?, Macromolecules 48 (7) (2015) 2224–2234
[33] S.B. Abbott, W.M. de Vos, L.L.E. Mears, M. Skoda, R. Dalgliesh, S. Edmondson, R. M. Richardson, S.W. Prescott, Switching the Interpenetration of Confined Asymmetric Polymer Brushes, Macromolecules 49 (11) (2016) 4349–4357.
[34] I.J. Gresham, B.A. Humphreys, J.D. Willott, E.C. Johnson, T.J. Murdoch, G.B. Webber, E.J. Wanless, A.R.J. Nelson, S.W. Prescott, Geometrical Confinement Modulates the Thermoresponse of a Poly(N-isopropylacrylamide) Brush, Macromolecules 54 (5) (2021) 2541–2550.
[35] L.L.E. Mears, S.B. Abbott, R.D. Barker, W.M. de Vos, S.W. Prescott, R.M. Richardson, Structural Evidence for a Reinforcing Response and Retention of Hydration During Confinement of Cartilage Lipids, Front. Phys. 9 (2021), https://doi.org/10.3389/fphy.2021.703472.
[36] L. Lindh et al., Salivary pellicles, Monogr. Oral Sci. 24 (2014) 30–39.
[37] C. Wickström, G. Svensäter, Salivary gel-forming mucin MUC5B–a nutrient for dental plaque bacteria, Oral Microbiol. Immunol. 23 (3) (2008) 177–182.
[38] B.D. Raynal et al., Calcium-dependent protein interactions in MUC5B provide reversible cross-links in salivary mucus, J. Biol. Chem. 278 (31) (2003) 28703–28710.
[39] C. Wickström, J.R. Davies, G.V. Eriksen, E.C.I. Veerman, I. Carlstedt, MUC5B is a major gel-forming, oligomeric mucin from human salivary gland, respiratory tract and endocervix: identification of glycoforms and C-terminal cleavage, Biochem. J. 334 (3) (1998) 685–693.
[40] J. Sotres et al., NanoWear of Salivary Films vs Substratum Wettability, J. Dent. Res. 91 (10) (2012) 973–978.
[41] T. Saerbeck, R. Cubitt, A. Wildes, G. Manzin, K.H. Andersen, P. Gutfreund, Recent upgrades of the neutron reflectometer D17 at ILL, J. Appl. Cryst. 51 (2) (2018) 249–256.
[42] J. Webster, S. Holt, R. Dalgliesh, INTER the chemical interfaces reflectometer on target station 2 at ISIS, Physica B Condens. Matter 385-386 (2006) 1164–1166.
[43] M. Born, E. Wolf, Principles of Optics, Pergamon Press, UK, 1970.
[44] A.J. Nelson, S. Prescott, refnx: neutron and X-ray reflectometry analysis in Python, J. Appl. Crystallogr. 52 (1) (2019) 193–200.
[45] I.J. Gresham, D.M. Reurink, S.W. Prescott, A.R.J. Nelson, W.M. de Vos, J.D. Willott, Structure and Hydration of Asymmetric Polyelectrolyte Multilayers as Studied by Neutron Reflectometry: Connecting Multilayer Structure to Superior Membrane Performance, Macromolecules 53 (23) (2020) 10644–10654.
[46] I. Horcas et al., WSXM: A software for scanning probe microscopy and a tool for nanotechnology, Rev. Sci. Instrum. 78 (1) (2007) 013705.
[47] J. Sotres, A.M. Baró, AFM imaging and analysis of electrostatic double layer forces on single DNA molecules, Biophys. J. 98 (9) (2010) 1995–2004.
[48] H.-J. Butt, M. Jaschke, Calculation of thermal noise in atomic force microscopy, Nanotechnology 6 (1) (1995) 1–7.
[49] L. Lindh et al., Adsorption of MUC5B and the role of mucins in early salivary film formation, Colloids Surf. B 25 (2) (2002) 139–146.
[50] V. Rondelli et al., Mucin Thin Layers: A Model for Mucus-Covered Tissues, Int. J. Mol. Sci. 20 (15) (2019) 3712, https://doi.org/10.3390/ijms20153712.
[51] H.-J. Butt, B. Cappella, M. Kappl, Force measurements with the atomic force microscope: Technique, interpretation and applications, Surf. Sci. Rep. 59 (1) (2005) 1–152.
[52] J. Kieser, B. Singh, M. Swain, I. Ichim, J.N. Waddell, D. Kennedy, K. Foster, V. Livingstone, Measuring intraoral pressure: adaptation of a dental appliance allows measurement during function, Dysphagia 23 (3) (2008) 237–243.
[53] M. Yoshikawa, M. Yoshida, K. Tsuga, Y. Akagawa, M.E. Groher, Comparison of three types of tongue pressure measurement devices, Dysphagia 26 (3) (2011) 232–237.
[54] W. Aroonsang et al., Influence of substratum hydrophobicity on salivary pellicles: organization or composition?, Biofouling 30 (9) (2014) 1123–1132
[55] A. Alkan et al., The effect of periodontal surgery on bite force, occlusal contact area and bite pressure, J. Am. Dent. Assoc. 137 (7) (2006) 978–983.
[56] O. Hidaka et al., Influence of Clenching Intensity on Bite Force Balance, Occlusal Contact Area, and Average Bite Pressure, J. Dent. Res. 78 (7) (1999) 1336–1344.